



Lining Structure of Water Conveyance Tunnel under Earthquake Action Research on Damage Law

Zhenxuan Gao ^{a*}

^a School of Civil and Transportation, North China University of Water Resources and Electric Power, Zhengzhou-450045, Henan, China.

Author's contribution

The sole author designed, analysed, interpreted and prepared the manuscript.

Article Information

DOI: <https://doi.org/10.9734/air/2024/v25i41099>

Open Peer Review History:

This journal follows the Advanced Open Peer Review policy. Identity of the Reviewers, Editor(s) and additional Reviewers, peer review comments, different versions of the manuscript, comments of the editors, etc are available here: <https://www.sdiarticle5.com/review-history/119169>

Original Research Article

Received: 24/04/2024

Accepted: 27/06/2024

Published: 01/07/2024

ABSTRACT

Based on the concrete damage plasticity constitutive model (CDP model) of ABAQUS software, the dynamic response of high pressure internal water conveyance tunnel during earthquake is simulated, and the dynamic response and dynamic damage law of high internal water pressure water conveyance tunnel structure under surrounding rock grade, buried depth and seismic wave intensity are analyzed. The research shows that the surrounding rock grade is closely related to the dynamic response and damage characteristics of the lining structure of the water conveyance tunnel. The dynamic damage of the tunnel under grade III surrounding rock is only 0.08, which is far less than 0.83 under grade IV surrounding rock. It can be considered that it will not cause great damage to grade III surrounding rock under earthquake. The surrounding rock grade is better, which can provide more stable support and reduce the stress and vibration of the structure. If the tunnel is in the seismic zone, the buried depth can be used as one of the design control indexes in the tunnel design. The lining damage is mainly distributed at the top and upper arch waist of the

*Corresponding author: E-mail: gaohizoxvn@163.com;

tunnel. With the increase of the buried depth of the tunnel, the dynamic damage amount increases from 0.021 to 0.081, then to 0.085. the damage of the lining structure also increases. This may be because the deep buried tunnel is more constrained by the underground rock and soil layer, thereby reducing the transmission of seismic load. The change of seismic wave intensity can directly affect the damage characteristics of tunnel lining structure. The dynamic damage mainly occurs at the vault and arch waist, and the damage area expands from the vault and arch waist to the side wall and corner. The increase of seismic wave intensity will lead to dramatic changes in the stress of the structure, which will lead to more complex and serious damage.

Keywords: Water conveyance tunnel; dynamic response; rock grade; buried depth; seismic wave intensity; reliability.

1. INTRODUCTION

In recent years, with the rapid development of China's economy and the acceleration of urbanization, the demand for water resources has increased, and long-distance water conveyance tunnels have become one of the important ways to solve the imbalance of urban water resources and urban development needs [1-3]. Underground structures such as long-distance water conveyance tunnels also appear in various regions of China. As an important part of the construction of hydraulic facilities, tunnels play an important role in the development of national economy and the construction of long-distance water transport in cities. Although China is still continuing to promote the innovation and development of science and technology and theory of tunnels, due to the complexity and diversity of geological structures in China's territory, including two major seismic zones, fold zones, fault zones, etc., the construction of long-distance water conveyance tunnels needs to pass through these geological structures, which is prone to increase the risk of geological disasters. At the same time, China is a mountainous country, and the earthquake risk in Southwest China, Northwest China and Qinghai-Tibet Plateau is high. The frequent activity of earthquakes can cause geological damage, especially in tunnels located in high-intensity seismic areas. The earthquake may affect the tunnel structure, including the damage of tunnel lining and payment structure under the action of seismic force, which threatens the safety and stability of tunnel structure [4-6]. Research at home and abroad shows that under the action of earthquake, the structure of long-distance water conveyance tunnel will be damaged to varying degrees, and multiple positions of tunnel lining may crack, resulting in disasters such as lining deformation and water seepage. A series of issues will affect the stability of the tunnel, resulting in a decline in the quality of long-

distance water delivery, and the efficiency of water delivery in the tunnel is greatly reduced. According to statistics, some water conveyance tunnels were damaged during the 1989 Northern California earthquake in the United States [7]. The earthquake caused the displacement of underground structures and geological deformation, which had a negative impact on the stability of water conveyance tunnels. The 2008 Wenchuan earthquake in China is a strong earthquake event in Chinese history [8]. The earthquake caused large-scale geological changes, and some of the tunnel linings cracked and the vault collapsed. In the 2016 New Zealand earthquake, a water conveyance tunnel in the earthquake area was seriously damaged [9]. The earthquake caused serious vertical displacement of the tunnel and had a serious impact on the underground infrastructure. The same situation occurred in the Kocaeli earthquake in Turkey [10], which not only caused thousands of deaths, but also triggered landslides and geological changes, causing damage to underground water delivery systems and tunnels. Although long-distance water conveyance tunnels are usually seismically designed and reinforced, areas with frequent seismic activity still need to be paid close attention to due to the possible impact of earthquakes on water conservancy projects, and measures need to be taken to improve the seismic capacity and safety of tunnel structures in response to possible future earthquake disasters to ensure the safety of people's lives and property [11-13].

This project is derived from the Guangdong Pearl River Delta Water Resources Allocation Project [14]. Here, the shield tunnel is 83.5 km long, and the length of the shield tunnel accounts for about 73.8 % of the total length of the line. Due to the requirements of the water supply system and pipeline layout, the water pipeline has to bear higher internal water pressure. The maximum

water radius of the water conveyance tunnel in this project is 6.4 m, and the maximum internal pressure of the water conveyance can reach 1.5 MPa. In order to ensure the safety of the project, the water conveyance tunnel uses composite lining, and the lining is prestressed to resist high internal water pressure.

Concrete constitutive model: The constitutive model of concrete is a mathematical model describing the behavior of concrete materials under mechanical loading. It includes the strength, deformation and damage characteristics of the material, which is used to simulate the mechanical response and failure process of concrete under different loading conditions. The constitutive model of concrete can be used to simulate the whole range of behavior from slight deformation to failure. In general, the constitutive model of concrete can be divided into two categories: linear and nonlinear, depending on whether the description of material behavior considers nonlinear effects [15]. Therefore, when establishing the constitutive relationship of concrete, it is necessary to consider the nonlinear effects and whether the strength, stiffness, deformation and damage of the material are reasonably expressed. Typical constitutive models include elastic model, elastic-plastic model and constitutive damage model. The elastic model assumes that the concrete has linear elastic behavior, that is, it follows Hooke's law during loading and unloading. The elastoplastic model takes into account the inelastic behavior of concrete and can describe the plastic deformation when it reaches a certain stress. The constitutive damage model is more complex, considering the damage accumulation and failure process of concrete [16-18]. In this paper, the concrete damage plasticity constitutive model (CDP model) of ABAQUS software is adopted for analysis and research.

According to the theory of plastic damage model, The total strain tensor ε consists of the elastic strain rate ε^{el} and the equivalent plastic strain rate ε^{pl} :

$$\varepsilon = \varepsilon^{el} + \varepsilon^{pl} \quad (1-1)$$

When the concrete is not damaged, the stress-strain relationship is:

$$\sigma = D^{el} (\varepsilon - \varepsilon^{pl}) \quad (1-2)$$

Where σ is the total stress and D^{el} is the elastic stiffness matrix.

When the concrete is damaged, the damage coefficient is introduced to characterize the weakening of the concrete stiffness. In the three-dimensional multi-axis state, the relationship between the damaged concrete can be described by the damage elastic equation:

$$\sigma = (1-d)\bar{\sigma} = (1-d)D^{el} (\varepsilon - \varepsilon^{pl}) \quad (1-3)$$

Where $\bar{\sigma}$ is the effective stress and d is the damage coefficient.

Under cyclic alternating stress, concrete will undergo a complex damage mechanism, which is due to the repeated changes of stress, strain and deformation caused by cyclic loading. There is a close relationship between damage factor and tensile and compressive damage variables, which are usually used to describe the damage degree and failure behavior of materials under stress. It is assumed that under alternating load, the relationship between damage factor and tensile and compressive damage variables is:

$$(1-d) = (1-s_t d_t)(1-s_c d_c), 0 \leq s_t, s_c \leq 1 \quad (1-4)$$

$$\begin{aligned} s_t &= 1 - w_t r^*(\bar{\sigma}), 0 \leq w_t \leq 1 \\ s_c &= 1 - w_c (1 - r^*(\bar{\sigma})), 0 \leq w_c \leq 1 \end{aligned} \quad (1-5)$$

where $r^*(\bar{\sigma})$ is the weight factor of the principal stress relationship under multi-directional stress state:

$$r^*(\bar{\sigma}) = \frac{\sum_{i=1}^3 \langle \bar{\sigma}_i \rangle}{\sum_{i=1}^3 |\bar{\sigma}_i|}, 0 \leq r^*(\bar{\sigma}) \leq 1 \quad (1-6)$$

Where w_t and w_c is the stiffness recovery weight factor; $\bar{\sigma}_i$ is the principal stress component; $\langle \bullet \rangle$ can be described as $\langle x \rangle = (|x| + x) / 2$.

The expression of effective stress is:

$$F(\bar{\sigma}, \varepsilon^{pl}) = \frac{1}{1-\alpha} (\bar{q} - 3\alpha \bar{p} + \beta (\varepsilon^{pl}) \langle \bar{\sigma}_{\max} \rangle - \gamma \langle -\bar{\sigma}_{\max} \rangle) - \bar{\sigma}_c (\varepsilon^{pl}) \quad (1-7)$$

$$\alpha = \frac{(\sigma_{bo}/\sigma_{co}) - 1}{2(\sigma_{bo}/\sigma_{co}) - 1}, (0 \leq \alpha \leq 0.5)$$

$$\beta(\varepsilon^{pl}) = \frac{\bar{\sigma}_c(\varepsilon^{pl})}{\bar{\sigma}_t(\varepsilon^{pl})} (1 - \alpha) - (1 + \alpha)$$

$$\gamma = \frac{1(1 - K_c)}{2K_c - 1}, p = -\frac{1}{3} I : \bar{\sigma}$$

$$\bar{q} = \sqrt{\frac{3}{2} \bar{S}}, \bar{S} = \bar{p} I + \bar{\sigma}$$

(1-8)

Where α and γ are dimensionless constants; $\bar{\sigma}_{\max}$ is the maximum effective principal stress; p is the effective hydrostatic pressure; q is Mises equivalent stress; σ_{bo} is the initial yield stress; σ_{co} is non-equiaxial initial yield stress; K_c is the parameter of deviatoric stress plane yield curve. I is the unit matrix; \bar{S} is the effective deviatoric stress.

G is the Drucker-Prager hyperbolic formula, expressed as follows:

$$\dot{\varepsilon}^{pl} = \dot{\lambda} \frac{\partial G(\bar{\sigma})}{\partial \bar{\sigma}} \quad (1-9)$$

$$G = \sqrt{(\varepsilon \sigma_{to} \tan \psi)^2 + q^2} - \bar{p} \tan \psi \quad (1-10)$$

where $\dot{\lambda}$ is the plastic factor.

The CDP model assumes that the main reason for the failure of concrete materials is damage and plasticity, that is, under the action of the outside world, damage will occur inside the material, and plastic deformation will also increase, eventually leading to material failure. In the tensile yield stage, concrete will gradually lose its stiffness and strength, and begin to develop cracks and damage. This causes the concrete to become more susceptible to failure when subjected to greater tensile stress. On the contrary, in the compressive yield stage, the concrete material will undergo a strengthening process after bearing a certain compressive load, and its strength and stiffness may increase slightly. However, with further loading, it will eventually enter the softening stage, resulting in a sharp decline in strength and stiffness.

Therefore, the CDP model describes the failure behavior of concrete materials by distinguishing the behavior of concrete in tensile and compressive states and considering its damage process.

2. MECHANICAL MODEL AND CALCULATION PARAMETERS

2.1 Introduction of ABAQUS Finite Element Analysis Software

ABAQUS is a general finite element analysis software, its nonlinear problem simulation ability is very excellent. It is suitable for simulating solutions in various complex environments. Its material library provides a lot of materials for users to use, but also Allow user-defined to simulate special materials. The types of elements provided are the same as other finite element software (such as ANSYS) software, there are many kinds. It can simulate various geometric models and the mechanical properties of their materials. For example, beam element, solid element and shell element. Can simulate a lot of organic polymer materials, various metals and Concrete materials often used in buildings, etc. Provide visual meshing operation, you can choose the whole or Locally, and even divide the edges. The whole model can be cut and the model can be divided into multiple geometric models. It makes the division of the model more-simple, improves the quality of the model and the accuracy of the model calculation results. To improve. In addition to the displacement and stress-strain that need to be solved in conventional mechanics, ABAQUS can also use a variety of methods. Modules calculate problems in other fields. Such as fluid, mechanical and acoustic analysis. Subroutine expansion is also supported Users can also do secondary development based on PYTHON language.

Because of its excellent ability to simulate nonlinear problems, it is suitable for simulating solutions in various complex environments. Many fields have its place, and ABAQUS is used to analyze the aerospace field in many countries. Counting. For the same problem, ABAQUS/Standard or ABAQUS/Explicit can be used. Module to solve.

2.2 Mechanical Model

Seismic waves can be classified according to different parameters of ground motion, mainly

including acceleration seismic waves, velocity seismic waves and displacement seismic waves. These three seismic waves describe the different motion characteristics of the ground in seismic events. The most commonly used is acceleration seismic waves, which are very important for evaluating the seismic performance of structures and analyzing the structural response under seismic loads. In this paper, El-Centro wave is selected for research.

Taking the water resources allocation project in the Pearl River Delta of China as the research background, the surrounding rock-tunnel dynamic model is established by using ABAQUS software. In the model, the quadrilateral plane strain element is used for both soil and lining. This element is usually one of the elements commonly used in finite element analysis, which is used to model the structural response under dynamic loading such as earthquake. The Mohr-Coulomb yield criterion is used to describe the characteristics of formation materials.

The calculation range is: the length \times width \times height of the simulated soil is $100 \times 25.6 \times 100$ (m), and the tunnel is located at the central axis of the soil. The grid division of the overall calculation model is shown in Fig. 1, and the

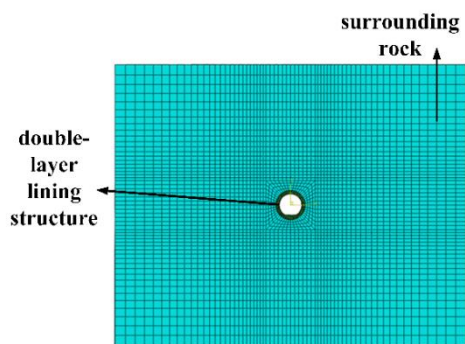


Fig. 1. Numerical model meshing

calculation model of the local water conveyance tunnel is shown in Fig. 2.

The selection of damage location in this paper should be based on the inherent strength of concrete materials. When the concrete material is subjected to excessive stress concentration in a certain local area, these areas are often more prone to damage. This is because the stress concentration will cause the stress in the region to far exceed the average stress of the material, thus reducing its bearing capacity. The potential hazards of local stress concentration are usually related to the degree and duration of stress concentration and the fatigue properties of materials. If the stress concentration exceeds the ultimate strength of the material, or the material is fatigued for too long, it will pose a threat to the safety of the structure.

2.3 Material Parameter

The corresponding physical and mechanical parameters of the surrounding rock grade of the calculation model are shown in Table 1; the corresponding physical and mechanical parameters of the lining are shown in Table 2, and the corresponding constitutive model parameters are shown in Table 3.

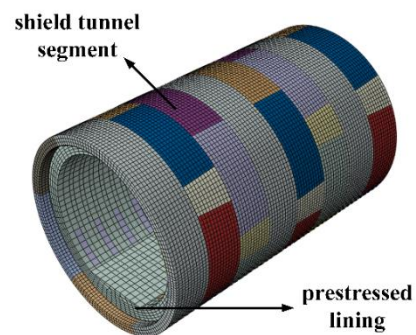


Fig. 2. Tunnel lining structure

Table 1. Physical and mechanical parameters of surrounding rock

Surrounding rock grade	Density $/(kg.m^{-3})$	Elastic modulus E/GPa	Poisson ratio ν	Aggregation force c/MPa
III	2620	7.25	0.29	1.15
IV	2580	2.13	0.35	0.60

Table 2. Physical and mechanical parameters of the lining structure

Concrete	Density $/(kg.m^{-3})$	Elastic modulus E/GPa	Poisson ratio ν	tensile strength f_t/MPa	compressive strength f_c/MPa
C50	2600	34	0.2	1.89	23.1

Table 3. ABAQUS input data—Plasticity

Expansion angle	Eccentricity ratio	f_{bd}/f_{c0}	K	Viscosity parameter
30	0.1	1.16	0.6667	0.006

Table 4. The relationship between damage parameter D and structural state

Overall description	Configuration status	Damage index D range
basically intact	locally slight	$0 \leq D < 0.10$
slight damage	overall slightly open	$0.10 \leq D < 0.30$
moderate damage	severe cracking, local spalling	$0.30 \leq D < 0.45$
severe damage	concrete broken	$0.45 \leq D < 0.95$
eventual failure	destruction, collapse	$D \geq 0.95$

2.4 Safety Assessment of Tunnel Lining

As an important part of the tunnel, when studying the influence of seismic load on the stability of tunnel structure, the stability of the tunnel can be judged by judging the damage coefficient of the lining structure, and the damage parameters of the lining can be more accurately judged.

In order to use the damage index to judge the state and performance level of concrete structure, it is necessary to divide the damage reasonably. The range of damage parameter D is also one of the most important problems in seismic design theory.

The concrete plastic damage model used in this analysis stipulates that the damage parameters are between $[0,1]$. When the concrete structure damage parameter $D = 0$, the structure is in a non-damage state; when $D \geq 0.95$, it can be considered that the unit fails, that is, the concrete loses its bearing capacity and is destroyed.

According to the existing test data and relevant regulations at home and abroad, combined with the concrete in this analysis by:

3. ANALYSIS OF SEISMIC DAMAGE CHARACTERISTICS OF TUNNEL

In order to study the damage law of lining structure of high internal water pressure water conveyance tunnel under earthquake, the damage plastic constitutive model (CDP) of

concrete in ABAQUS software is used to compare the dynamic response and dynamic damage of tunnel lining structure. The damage law of water conveyance tunnel lining under different influencing factors of surrounding rock grade, buried depth and seismic intensity is studied respectively.

3.1 Influence of Surrounding Rock Grade on Dynamic Loss of Tunnel

In this section, the influence of surrounding rock grade on the dynamic damage of tunnel lining structure will be analyzed under the condition of buried depth of 40 m and seismic intensity of 0.1g. The maximum values of dynamic response and dynamic damage under class III and IV surrounding rock grades are shown in Table 5.

From Table 5, it can be seen that with the increase of surrounding rock grade, the maximum value of minimum principal stress peak and the maximum value of maximum principal stress peak also increase. The maximum value of the minimum principal stress peak under the grade IV surrounding rock is 1.17 times that of the grade III surrounding rock, and the maximum value of the maximum principal stress peak is 2.98 times that of the latter. For concrete structures, their ability to withstand tensile stress is much lower than their ability to withstand compression, so large tensile stress can easily lead to concrete damage.

Table 5. The maximum dynamic response and damage quantity under two different grades of surrounding rock

Surrounding rock grade	Minimum principal stress/MPa	Maximum peak value of maximum principal stress /MPa	Peak acceleration / ($m \cdot s^{-2}$)	Maximum dynamic damage
III	-16.15	0.63	0.48	0.08
IV	-18.95	1.88	0.88	0.83

The acceleration time history curve at the left arch waist of the lining structure under the two surrounding rock grades is shown in Fig. 3. From Fig. 3, it can be seen that the acceleration time history curves of the two surrounding rock grades are basically the same in morphological characteristics, but the maximum peak acceleration of the structure under the grade III surrounding rock is 0.48 m/s^2 and occurs at 3.56 s, and the maximum peak acceleration of the structure under the grade IV surrounding rock is 0.88 m/s^2 , which is about 1.83 s times that of the former, and the time occurs at 4.04 s. When the surrounding rock grade gradually increases, the maximum peak acceleration of the corresponding lining structure occurs. The delay in time indicates that different engineering geological grades have a certain degree of influence on the transmission of seismic waves.

The distribution of dynamic damage of lining structure under grade III and IV surrounding rock is shown in the Fig. 4.

From the distribution of lining damage in Fig. 4, the damage distribution of tunnel structure in grade III surrounding rock is mainly concentrated at the top. With the improvement of the grade of surrounding rock, the damage and failure gradually transfer to the arch waist, and finally reach the destruction. The dynamic damage of the tunnel under the surrounding rock of grade III is only 0.08, which is much smaller than the dynamic damage of 0.83 under the surrounding

rock of grade IV. In the tunnel lining structure in the grade IV surrounding rock, it can be clearly seen that some of the lining has been damaged. Under the earthquake of 0.100 g, the tensile damage of grade IV surrounding rock under the lining structure is much larger than that of grade III surrounding rock, and the damage value appears earlier than that of grade III surrounding rock. This finding shows that the grade of surrounding rock has a significant influence on the seismic performance of tunnel structure. The tunnel lining structure under grade III surrounding rock is less damaged under earthquake, indicating that the surrounding rock grade is better, which can provide more stable support and reduce the stress and vibration of the structure. In contrast, the dynamic damage of tunnel lining structure under grade IV surrounding rock is larger, indicating that the grade of surrounding rock is poor, which makes the structure more susceptible to earthquake and damage.

3.2 Influence of Buried Depth on Dynamic Loss of Tunnel

The total buried depth of the calculation model is 80 m, and 20 m, 40 m and 60 m are selected as the buried depth research objects respectively. The variation law of the maximum dynamic response and dynamic damage of the lining structure with the buried depth of the tunnel is shown in Fig. 5.

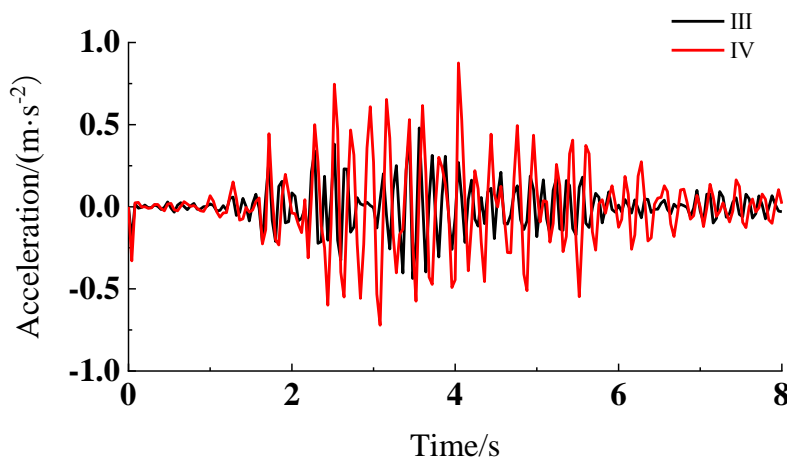


Fig. 3. Acceleration time history curves at the crown of the lining structure under two different grades of surrounding rock

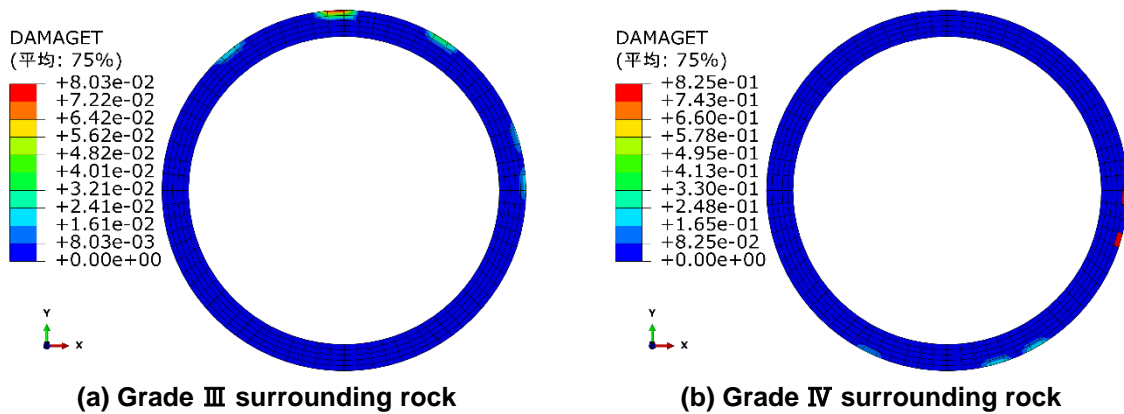


Fig. 4. Distribution of dynamic damage quantity in the lining structure under different grades of surrounding rock

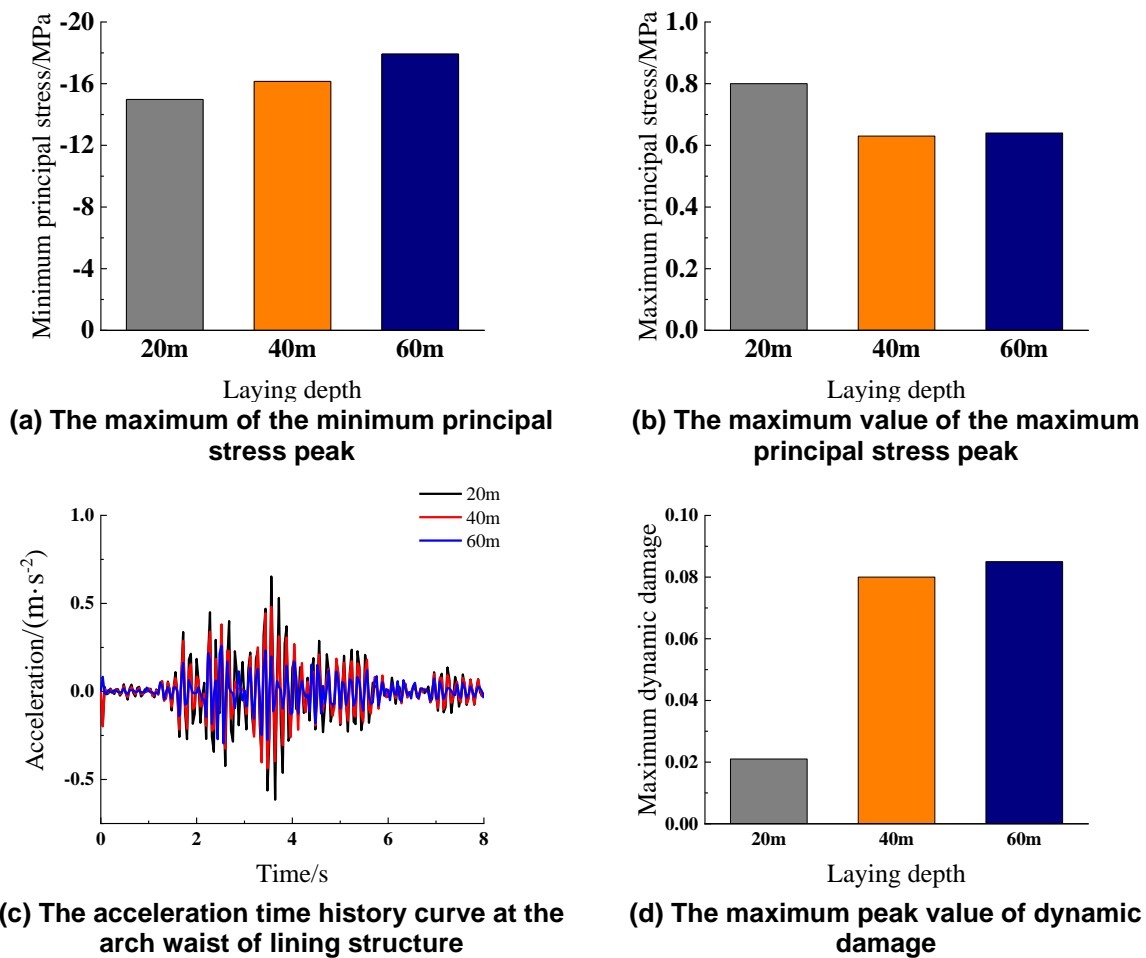


Fig. 5. The trend of maximum dynamic response and maximum dynamic damage quantity with varying depth of tunnel embedding

It can be seen from Fig.6 that with the increase of buried depth, the maximum value of the minimum principal stress peak and the dynamic damage of the lining structure show a non-linear

increasing trend, while the maximum principal stress peak shows a trend of decreasing first and increasing, and the decrease is far greater than the increase. The actual seismic damage data

show that the seismic damage degree of rock tunnel with buried depth greater than 50 m is obviously reduced. According to the calculation results of this paper, with the increase of buried depth, the dynamic response index of tunnel structure-peak acceleration decreases rapidly. The increase of the buried depth of the tunnel may reduce the influence of the earthquake on the structure. This may be because the deep buried tunnel is more constrained by the underground rock and soil layer, thus reducing the transmission of seismic load.

The distribution of lining dynamic damage under different tunnel buried depths is shown in the Fig. 6.

The dynamic damage distribution map of the tunnel buried depth of 20 m is shown in Fig. 6 (a). From the distribution area of lining damage, the dynamic damage area of the structure is mainly distributed at the top of the tunnel and the upper arch waist. With the increase of the buried depth of the tunnel, the damage of the lining structure also increases, and the damage area is larger. Specifically, from 20 m buried depth to 40 m, the dynamic damage increased from 0.021 to 0.081, with an increase of 3.86 times. However, from 40 m to 60 m, the dynamic damage increased from 0.081 to 0.085, with an increase of 1.05 times, which was significantly lower than that of the former. At the buried depth of 20 m, the lining structure did not undergo tensile damage at the beginning, and with the increase of the buried depth, the time of tensile damage appeared earlier and earlier. When the buried depth is 40 m and 60 m, the tensile damage first increases rapidly and then the growth rate slows

down to reach the maximum damage value, and the maximum tensile damage curves of the two are similar.

When the buried depth is 40m to 60m, the growth rate of the maximum loss decreases rapidly, but after 50m, with the increase of the buried depth, the growth rate of the maximum loss decreases or even the maximum loss decreases. When the tunnel is located in the weak stratum or the buried depth is shallow, the possibility and severity of earthquake damage are high in theory. Especially when the buried depth is less than 50 m, the earthquake damage is more serious. When the tunnel is located in the weak stratum or the buried depth is shallow, the possibility and severity of earthquake damage are high in theory. Especially when the buried depth is less than 50 m, the earthquake damage is more serious. This is because the greater the buried depth of the tunnel, the stronger the constraint of the stratum, and the smaller the possibility of earthquake damage in theory.

In the surrounding rock with good lithology, the greater the buried depth of the tunnel structure, the smaller the energy transmitted from the seismic surface wave, and the corresponding reduction of tunnel seismic damage. The greater the buried depth of the tunnel is, the stronger the constraint of the stratum is, and the less likely the earthquake damage is in theory. In the surrounding rock with good lithology, the greater the buried depth of the tunnel structure, the smaller the energy transmitted from the seismic surface wave, and the corresponding reduction of tunnel seismic damage.

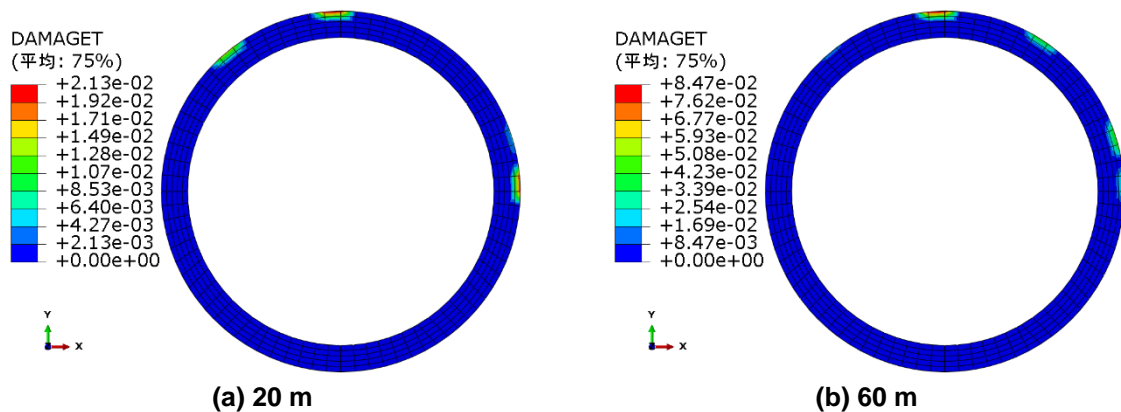


Fig. 6. Distribution of dynamic damage quantity in the lining structure under different embedding depths

3.3 Influence of Seismic Wave Intensity on Dynamic Loss of Tunnel

Seismic wave intensity is a physical quantity that describes the energy of seismic waves during propagation. In seismology, the intensity of seismic waves is usually measured by Peak Ground Acceleration (PGA), that is, the maximum acceleration value generated by seismic waves at a certain point on the ground. In this paper, the surrounding rock of grade III and the buried depth of 40 m are selected as the research background, and the peak acceleration of seismic wave is 0.075 g, 0.100 g, 0.150 g and 0.200 g as the research object. The dynamic response of lining structure and the maximum value of dynamic damage with the change of seismic wave intensity calculated by the model are shown in Fig. 7.

It can be seen from Fig. 7 that with the increase of seismic wave intensity, the peak value of minimum principal stress, the peak value of left haunch acceleration and the maximum value of

maximum dynamic damage all show a non-linear increasing trend, while the peak value of maximum principal stress shows a gradual decreasing trend. When the peak acceleration is 0.200 g, the maximum compressive principal stress of the structural lining reaches 22.77 MPa, which is equivalent to 98% of the design value of concrete compressive strength. However, in view of the influence of damage on concrete, the tensile and compressive strength limits of concrete need to be reduced accordingly. When the dynamic damage reaches 0.1, the maximum compressive stress of lining is very likely to reach the compressive design strength of concrete, which indicates that with the increase of seismic wave strength, the structure may face more severe challenges. Therefore, in the process of design and construction, the influence of seismic wave intensity on the structure must be fully considered, and corresponding seismic design measures should be taken into consideration to ensure the safety and stability of the structure under earthquake conditions.

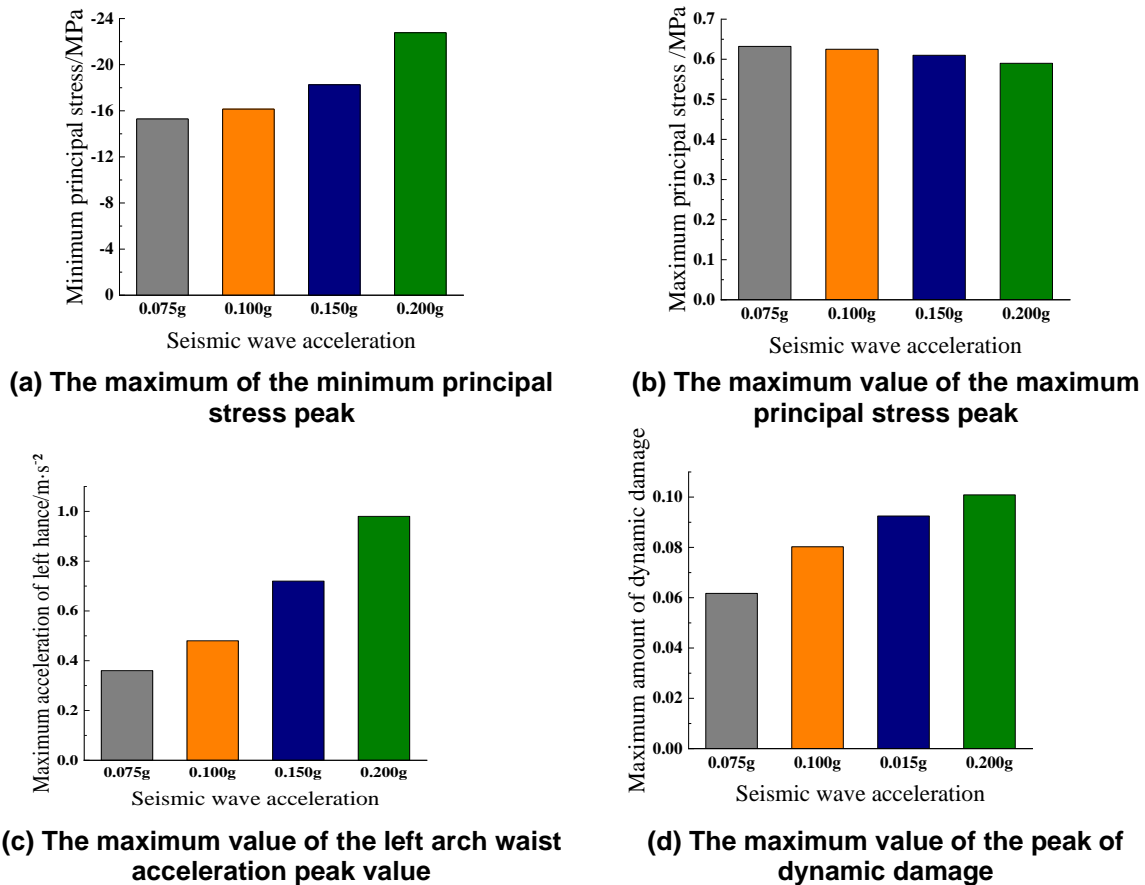


Fig. 7. The pattern of maximum dynamic response and maximum dynamic damage quantity with varying seismic wave intensity

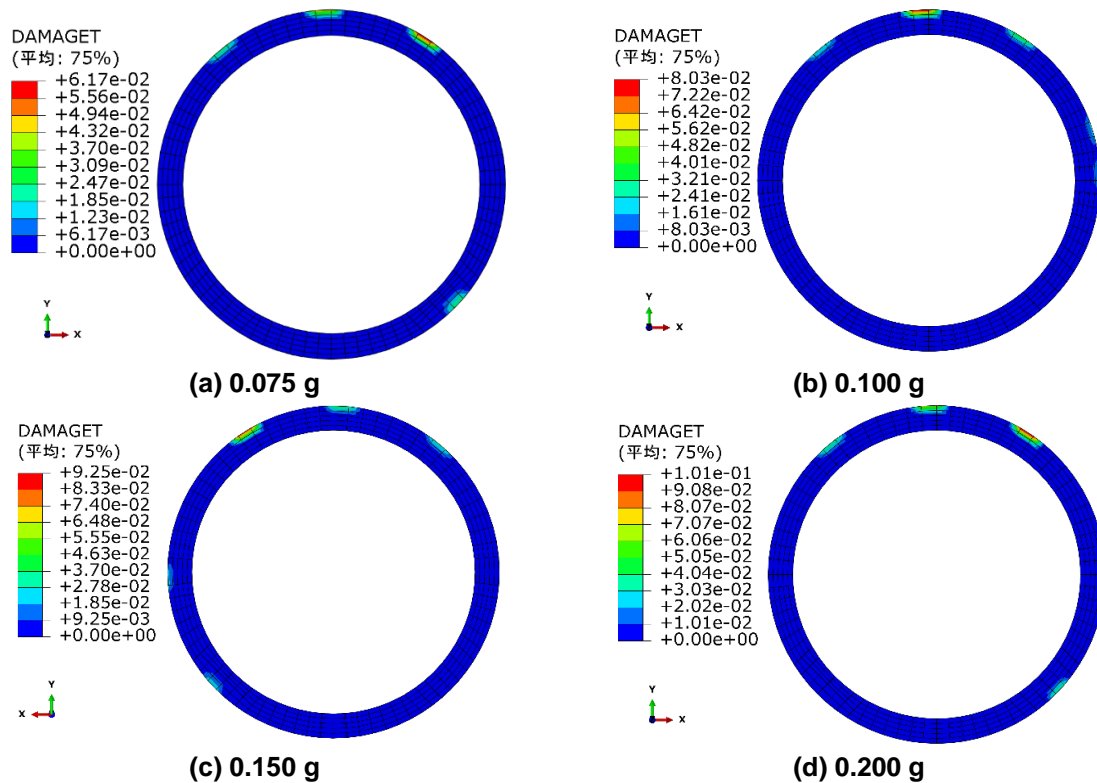


Fig. 8. Distribution of dynamic damage quantity in the lining structure under different seismic wave intensities

It can be seen from Fig. 8 that when the peak acceleration of the earthquake is 0.075 g, the damage of the tunnel lining mainly occurs at the vault and the left and right haunches, and there is also a small damage at the right wall corner, while the maximum dynamic damage mainly occurs at the right haunch. When the peak acceleration of seismic wave reaches 0.100 g, the maximum dynamic damage of tunnel lining appears at the vault, and the dynamic damage increases compared with 0.075 g, while the right wall and corner begin to appear smaller damage area. As the peak acceleration of seismic wave gradually increases to 0.150 g and 0.200 g, the dynamic damage amount of the damage zone of the tunnel lining structure increases. The damage is mainly concentrated at the vault and arch waist of the lining structure, and the damage zone extends from the vault and arch waist to the side wall and corner. When the seismic wave intensity is 0.150 g and 0.200 g, the lining structure rapidly occurs tensile damage and reaches the maximum tensile damage. In the case of 0.075 g and 0.100 g, the lining structure first undergoes rapid tensile damage and then the damage growth rate slows down and finally reaches the maximum tensile damage.

4. CONCLUSION

By using the CDP constitutive model of ABAQUS, the lining structure of the high internal water pressure water conveyance tunnel in the Pearl River Delta water resources allocation process is studied. The influence of surrounding rock grade, buried depth and seismic wave intensity on the dynamic characteristics and dynamic damage characteristics of the lining structure of the water conveyance tunnel is analyzed. The following conclusions are obtained:

- 1) The grade of surrounding rock is closely related to the dynamic response and damage characteristics of the lining structure of the water conveyance tunnel. The maximum value of dynamic damage in grade IV surrounding rock is 10.38 times that of grade III surrounding rock. It can be considered that the lining structure will not be greatly damaged under the grade III surrounding rock, while the lining structure damage under the grade IV surrounding rock mainly occurs in the side wall position and causes obvious damage. The

surrounding rock grade is better, which can provide more stable support and reduce the stress and vibration of the structure.

- 2) With the increase of buried depth, the dynamic response index of tunnel structure-peak acceleration decreases rapidly, while the maximum principal stress, the maximum peak value of minimum principal stress of lining structure increase nonlinearly. From 20 m to 40 m, the dynamic damage increased from 0.021 to 0.081, with an increase of 3.86 times. However, from 40 m to 60 m, the dynamic damage increased from 0.081 to 0.085, with an increase of 1.05 times, which was significantly smaller than the former. The increase of the buried depth of the tunnel may reduce the influence of the earthquake on the structure.
- 3) The strength of seismic wave directly affects the seismic force of tunnel lining structure, and then determines the degree of seismic response and dynamic damage characteristics. When the peak acceleration is 0.200 g, the maximum compressive stress of the structural lining is 22.77 MPa, which is 98% of the compressive design strength of concrete. However, in view of the influence of damage on concrete, the tensile and compressive principal stresses of concrete need to be reduced, so the damage position of the structural lining is prone to compressive failure. With the increase of seismic wave intensity, the dynamic damage of tunnel lining structure increases nonlinearly. This is because the increase of seismic wave intensity will lead to the dramatic change of structural stress, which will lead to more complex and serious damage.

DISCLAIMER (ARTIFICIAL INTELLIGENCE)

Author(s) hereby declare that NO generative AI technologies such as Large Language Models (ChatGPT, COPILOT, etc) and text-to-image generators have been used during writing or editing of manuscripts.

COMPETING INTERESTS

Author has declared that no competing interests exist.

REFERENCES

1. Xie W Q, Li W W, Liu X L, et al. In-situ methods for the TBM dismantling in a long-

distance and deep-buried tunnel: Case study of Xinjiang water conveyance tunnel[J]. *Tunnelling and Underground Space Technology*. 2022;129:104683.

2. Duan K, Zhang G, Sun H. Construction practice of water conveyance tunnel among complex geotechnical conditions: a case study[J]. *Scientific Reports*. 2023; 13(1):15037.
3. Chen Z, Yu H, Yuan Y. Full 3D seismic analysis of a long-distance water conveyance tunnel[J]. *Structure and Infrastructure Engineering*. 2014;10(1): 128-140.
4. Qu Z, Zhu B, Cao Y, et al. Rapid report of seismic damage to buildings in the 2022 M 6.8 Luding earthquake, China[J]. *Earthquake Research Advances*. 2023;3(1):100180.
5. Baker J, Bradley B, Stafford P. *Seismic hazard and risk analysis*[M]. Cambridge University Press; 2021.
6. Danciu L, Nandan S, Reyes CG, et al. The 2020 update of the European Seismic Hazard Model-ESHM20: Model overview[J]. *EFEHR Technical Report*. 2021;1.
7. Hauksson E, Stock J, Hutton K, et al. The 2010 M w 7.2 el mayor-cucapah earthquake sequence, Baja California, Mexico and southernmost California, USA: Active seismotectonics along the Mexican pacific margin[J]. *Pure and Applied Geophysics*. 2011;168:1255-1277.
8. Bai S, Wang J, Zhang Z, et al. Combined landslide susceptibility mapping after Wenchuan earthquake at the Zhouqu segment in the Bailongjiang Basin, China[J]. *Catena*. 2012;99:18-25.
9. Kaiser A, Balfour N, Fry B et al. The 2016 Kaikōura, New Zealand, earthquake: Preliminary seismological report[J]. *Seismological Research Letters*. 2017; 88(3):727-739.
10. Flora A, Chiaradonna A, de Sanctis L, et al. Understanding the damages caused by the 1999 Kocaeli earthquake on one of the towers of the theodosian walls of constantinople[J]. *International Journal of Architectural Heritage*. 2022;16(7):1076-1100.
11. Zakian P, Kaveh A. Seismic design optimization of engineering structures: A comprehensive review[J]. *Acta Mechanica*. 2023;234(4):1305-1330.
12. Koseki J, Tateyama M, Shinoda M. Seismic design of geosynthetic reinforced

- soils for railway structures in Japan[M]//New Horizons in Earth Reinforcement. CRC Press. 2023;113-119.
13. Leyva H, Bojórquez J, Bojórquez E, et al. Multi-objective seismic design of BRBs-reinforced concrete buildings using genetic algorithms[J]. Structural and Multidisciplinary Optimization. 2021;64(4): 2097-2112.
 14. Wang J, Yang S, Xu X, et al. 3C-3D tunnel seismic reverse time migration imaging: A case study of Pearl River Delta Water Resources Allocation Project[J]. Journal of Applied Geophysics. 2023;210:104954.
 15. Voyiadjis G Z, Taqieddin Z N. Elastic plastic and damage model for concrete materials: Part I-theoretical formulation[J]. The International Journal of Structural Changes in Solids. 2009;1(1): 31-59.
 16. Lu D, Du X, Wang G, et al. A three-dimensional elastoplastic constitutive model for concrete[J]. Computers & Structures. 2016;163:41-55.
 17. Jankowiak T, Lodygowski T. Identification of parameters of concrete damage plasticity constitutive model[J]. Foundations of Civil and Environmental Engineering. 2005;6(1):53-69.
 18. Ouyang X, Wu Z, Shan B, et al. A critical review on compressive behavior and empirical constitutive models of concrete[J]. Construction and Building Materials. 2022;323:126572.

Disclaimer/Publisher's Note: The statements, opinions and data contained in all publications are solely those of the individual author(s) and contributor(s) and not of the publisher and/or the editor(s). This publisher and/or the editor(s) disclaim responsibility for any injury to people or property resulting from any ideas, methods, instructions or products referred to in the content.

© Copyright (2024): Author(s). The licensee is the journal publisher. This is an Open Access article distributed under the terms of the Creative Commons Attribution License (<http://creativecommons.org/licenses/by/4.0>), which permits unrestricted use, distribution, and reproduction in any medium, provided the original work is properly cited.

Peer-review history:

The peer review history for this paper can be accessed here:

<https://www.sdiarticle5.com/review-history/119169>